J. Plasma Physics (1997), *vol.* 57, *part* 1, *pp.* 203–229

Experimental evidence of rapid relaxation to large-scale structures in turbulent fluids: selective decay and maximal entropy

MICHAEL R. BROWN

Department of Physics and Astronomy, Swarthmore College, Swarthmore, Pennsylvania 19081, USA

(Received 2 May 1996)

There is abundant experimental, theoretical and computational evidence that certain constrained turbulent fluid systems self-organize into large-scale structures. Examples include two-dimensional (geostrophic) fluids, guiding-centre plasmas and pure-electron plasmas, as well as two- and three-dimensional magnetofluids such as reversed-field pinches and spheromaks. The theoretical understanding of relaxation phenomena is divided into two quite different constructs: selective decay and maximal entropy. Theoretical foundations of both of these principles are largely due to Montgomery and his collaborators. In this paper, selective decay and maximal entropy theories of turbulent relaxation of fluids are reviewed and experimental evidence is presented. Experimental evidence from both 2D fluids and from 3D magnetofluids is consistent with the selective decay hypothesis. However, high-resolution computational evidence strongly suggests that formation of large-scale structures is dictated by maximal-entropy principles rather than selective decay.

1. Introduction

There is abundant evidence that certain constrained turbulent fluid systems self-organize or relax into large-scale structures. These include two-dimensional (or geostrophic) fluids such as hurricanes on Earth and the Great Red Spot on Jupiter, guiding-centre plasmas and pure electron plasmas, as well as two- and three-dimensional magnetofluids such as reversed-field pinches and spheromaks. The current theoretical understanding of relaxation phenomena is divided into two quite different constructs both developed largely by Montgomery and his collaborators: selective decay (Montgomery *et al.* 1978; Matthaeus and Montgomery 1980) and maximal entropy (Joyce and Montgomery 1973; Montgomery and Joyce 1974; Montgomery *et al.* 1979).

The selective decay hypothesis is characterized by the following. If one considers the 'ideal invariants' of the system and admits a small amount of dissipation, it is often found that one of the invariants is 'better conserved' or more rugged than others. If one minimizes the expression for the poorly conserved invariant subject to the constraint that the rugged invariant is conserved using the technique of Lagrange multipliers, an Euler equation for the field variables results. The Lagrange multiplier is the ratio of the poorly conserved invariant to the ruggedly conserved one. The main drawback of the hypothesis is that it often requires many characteristic

times for the selectively decayed state to emerge. Experimentally and computationally it is observed that large-scale structures can form in times comparable to a characteristic time of the flow. In the following sections, we shall discuss selective decay of enstrophy-to-energy for two-dimensional Navier–Stokes flows (2D NS), of energy-to-mean square vector potential for two-dimensional magnetohydrodynamics (2D MHD), and of energy-to-helicity for three-dimensional magnetohydrodynamics (3D MHD).

The principle of maximal entropy dictates that the air in a room initially distributed in clumps moves towards smooth uniformity; thermodynamic equilibrium does not admit-large scale structures. However, for a system with a constrained phase space, maximal entropy can generate large-scale structures as a long-lived intermediate state. To apply the principle of maximal entropy, one needs to consider a discrete or quantized version of the field variables. If we have N such quanta of the field (vortices in the case of 2D flow, bundles of flux or current filaments in the case of MHD, or individual spins in the case of the 2D spin system), we consider the number of ways these N quanta can be arranged in a given state (say spins up or down). The Boltzmann entropy is defined as $S = k \ln \Omega$, i.e. the logarithm of the number of permutations. The most probable state is the one with the most permutations or the highest entropy subject to other constraints (such as conservation of energy and particle number). The maximal-entropy perspective addresses the question: are these observed large-scale, self-organized structures in some sense statistically more probable than other less simple ones?

Strictly speaking, selective-decay and maximal-entropy methods apply only to isolated systems. It is for this reason that we shall concentrate on systems that are freely decaying or are otherwise disconnected from external energy sources. The situation is more complicated for driven systems, though many of the features found in isolated systems carry over. Fusion magnetofluids require external driving (if only for current drive and fuelling), so it is important in this case to understand the features of driven, steady-state turbulent magnetofluids. The statement of the problem is simple: what happens to a cylinder of dissipative magnetofluid when you apply a voltage between the ends? A few features emerge from simulations (Montgomery 1989; Dahlburg *et al.* 1988; Hossain *et al.* 1983; Hossain 1994). Within a few tens of characteristic times (Alfvén times), a quasi-time-independent, relaxed state is established (very much like the undriven decay case). The relaxed state is characterized by the formation of a large-scale structure (a helically deformed current channel) and significant organized flow. Large-scale flow patterns have been observed in steady-state driven tokamaks (Tynan *et al.* 1992). Associated with the formation of large scale structure is the back-transfer or inverse cascade of certain ideal invariants in the Fourier representation. The selective accumulation of some ideal invariant at the largest scale admitted by the boundary conditions (energy in 2D NS, mean square vector potential in 2D MHD and helicity in 3D MHD) is related to the selective decay of another ideal invariant in the non-driven case (enstrophy in 2D NS, and energy in 2D and 3D MHD). Further discussion of driven fluid systems is outside the scope of this review.

We should like to focus attention on a few fluid or continuous medium systems: the two-state spin system (Sec. 2), the two-dimensional Navier–Stokes (2D NS) system (Sec. 3) and the two- and three-dimensional magnetohydrodynamic systems (2D and 3D MHD) (Sec. 4). There are several features common to each (see Table 1). First, they self-organize or relax to large-scale structures, i.e. to structures as large

Table 1. Comparison of statistical systems that exhibit relaxation to large scales.

	Two-state spin system	2D Navier–Stokes and line-vortex system	3D MHD and current-filament system
Ideal invariants	E, N	Ω (direct cascade) E (inverse cascade)	E (direct cascade) H_c, K (inverse cascade) $\int a^2\, d^2x$ (inverse cascade in 2D)
Negative temperature?	Yes	Yes	β_E, $\beta_K < 0$?
Phase space limits	E bounded above and below for fixed N	E bounded above and below for fixed N	E_B bounded below for fixed K
Type of interaction	Point	Point/continuum	Continuum
Equilibration $t_{\rm eq}$	T_2	$t_{\rm eddy}$	$t_{\rm Alf}$
Dissipation $t_{\rm diss}$	T_1	$t_{\rm viscous}$	$t_{L/R}$
Theory	Ramsey	Onsager, Montgomery, Joyce, Matthaeus, Kraichnan	Frisch, Montgomery, Turner, Vahala, Matthaeus, Dahlburg
Experiment	Purcell, Pound, Abragam	Driscoll, Fine, Huang, Tabeling, Hopfinger	Barnes, Jarboe, Brown, Bodin

as allowed by boundary conditions. Secondly, the relaxation is rapid compared with a thermodynamic equilibration time or decay time. Often, the relaxation is as fast as the characteristic time of the flow (the interaction or eddy turnover time or Alfvén time for MHD). Thirdly, in each case, the dynamics and therefore the statistical phase space are constrained in some way. Because of the constrained phase space, these systems admit negative temperature and therefore an exponentially increasing Boltzmann factor. Fourthly, there are ideal invariants for each system, i.e. quantities that are conserved in the absence of dissipation. Further, if a small amount of dissipation is admitted, it is often the case that at least one of the ideal invariants is more strongly affected by the dissipation than the others.

2. Two-state spin system

In order to provide a framework for some of the statistical concepts to be used later, let us review a simple two-state spin system. Consider a two-dimensional array of N weakly interacting, localized spins in an external magnetic field with n_+ directed upward and n_- directed downward (Purcell and Pound 1951; Ramsey 1956; Abragam and Proctor 1957). An up spin contributes $+\mu B$ to the energy while a down spin contributes $-\mu B$ (the field is oriented downward). The energy of the system depends only on the number of excess up spins: $E = \mu B(n_+ - n_-)$. If all N spins are up, the system has its maximum energy $E_{\max} = N\mu B$.

We can write the number of distinct ways in which the N spins can be arranged for a given proportion of n_+ and n_-:

$$\Omega(n_+, n_-) = \frac{N!}{n_+!\, n_-!}. \tag{1}$$

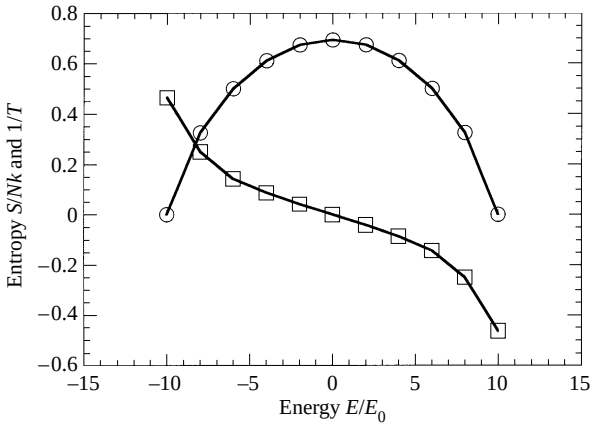

Figure 1. Plot of entropy and inverse temperaure versus energy for the two-state spin system for $N = 10$: ○ entropy in units of Nk, (2), □, $1/T = \partial S/\partial E$.

Note that there is only one way to construct the maximum- and minimum-energy states (all spins up or all spins down) and there are the most permutations with an equal proportion of up and down spins. The Boltzmann entropy of the system is defined as $S = k \ln \Omega$, so that the highest-entropy configuration corresponds to the one with the most permutations. If we use Stirling's approximation for the factorial ($\ln n! \approx n \ln n - n$), the entropy of our spin system can be written (in a suggestive way)

$$S = k \left(N \ln N - \sum_{+,-} n_i \ln n_i \right) = -k \sum_{+,-} n_i \ln n_i + \text{const}, \tag{2}$$

where the sum is taken over all the spins in the 2D array.

The quantity that equalizes when two systems are in equilibrium is defined as

$$\beta \equiv \frac{1}{kT} = \frac{1}{k} \left(\frac{\partial S}{\partial E} \right)_n ,$$

where T is the temperature. We can see that since there is a maximum energy and there is only one way to construct it, it follows that the spin temperature is formally negative for positive energies (see Fig. 1). Note also that the highest energy state is also the most ordered, and corresponds to $S = 0$.

The situation is quite different for an unconstrained system. Recall that for an ideal gas with an unlimited phase space, the number of distinct permutations grows with energy and number of degrees of freedom f like $E^f = E^{3N/2}$. The entropy $S = \frac{3}{2} Nk \ln E$, so $\beta = 3N/2E$ or $T = 2E/3Nk$. This is the intuitive result that for an ideal gas the temperature is always positive and grows with increasing average energy: $\bar{E} = \frac{3}{2} NkT$. Because the number of available states increases rapidly with energy (for conventional systems) and because we can assume ergodicity (all states equally likely), it follows there are many more states at higher energy and the probability of their occupation is lower. This is reflected in the Boltzmann factor $\exp(-E/kT)$. If phase space is constrained somehow and there are *fewer* states at higher energy then those states are *more* likely. This is the case of negative temperature, and is reflected in the Boltzmann factor $\exp(+E/kT)$.

There were a number of experiments performed on negative-temperature spin systems during the 1950s. Purcell and Pound (1951) performed experiments on LiF crystals in a strong magnetic field. The nuclear magnetization of an LiF sample was reversed by rapidly changing the sign of an applied magnetic field. They measured the cooling curve (via the ^{7}Li resonance) as the negative-temperature spin system slowly equilibrated with the positive-temperature lattice. It was pointed out by Ramsey (1956) that the negative-temperature state persists for a macroscopic time (several minutes), which he called T_1, but the relaxation time necessary to establish the negative temperature state was very short (a few microseconds), and was called T_2. T_1 is the thermodynamic time required for the spins to equilibrate with the lattice while T_2 is the characteristic time for the spin system (the Larmor precession time). Disparate time scales are an important ingredient for the establishment of large-scale structures.

This relatively simple system displays many of the principal ideas we shall draw upon later. First, the phase-space volume is limited, since there is either a maximum energy for the system or some other constraint. Secondly, because there is a maximum energy, the system admits a negative temperature. A formally negative temperature implies an exponentially growing Boltzmann factor. Thirdly, the negative temperature states exhibit large-scale order. Indeed, the phase transition that exists for interacting spins implies large-scale order. Finally, the large-scale order can persist for times long compared with a characteristic time scale for the system, but will eventually decay on thermodynamic times.

3. Two-dimensional Navier–Stokes flow and line vortices

We now turn our attention to a fluid system where the entities are no longer fixed to a lattice but are free to move. To stay as close as possible to the 2D spin system, let us first consider a 2D magnetized plasma consisting of a collection of N charged rods of mass m, n_+ of them charged positively and n_- charged negatively. The magnetic field is applied along the length of the rods. The equation of motion for a given rod (which we label j) is

$$\frac{d\mathbf{v}_j}{dt} = \frac{q_j}{m}(\mathbf{E}_j + \mathbf{v}_j \times \mathbf{B}), \tag{3}$$

where q_j is the charge of the rod. Recall that in the case of the two-state spin system, the energy is due to interaction of the entities with an external field, and the entities are fixed on a lattice. In the case of the 2D rod plasma, energy is due to interaction among the entities (or equivalently a mean field) and the entities are free to move. Clearly, for a given fixed configuration of rods, the highest-energy states can be obtained if all the rods are the same sign (analogous to all the spins up). However, for a fixed proportion of n_+ and n_- (say $n_+ = n_-$), the highest-energy states are characterized by clumping all the positive rods together and all the negative rods together and then separating the clumps as far as possible. If we demand that the system is in a high-energy state then like-signed rods must clump together just as all the spins must flip up to form a high-energy state in the 2D spin system.

The dynamics of the 2D plasma is simplified if we invoke the 'guiding centre' approximation. We can average over the high-frequency cyclotron motion of the rods (effectively neglecting the left-hand side of (3)) and retain only the slow drift

motion, so that $\mathbf{E} + \mathbf{v} \times \mathbf{B} = 0$ and $\mathbf{E} \cdot \mathbf{B} = 0$, so

$$\mathbf{v}_j = \frac{\mathbf{E}_j \times \mathbf{B}}{B^2}. \tag{4}$$

Interesting connections can be established between the continuous and discrete models of the guiding-centre plasma and 2D Navier–Stokes fluids. If one takes a fluid limit of the guiding-centre plasma (continuous charge distribution), it can be shown that the equations are isomorphic to the 2D Navier–Stokes equations (Montgomery and Joyce 1974; Montgomery 1975). Conversely, one can arrive at a discrete-vortex model for 2D fluid flow in which vorticity is permanently concentrated into delta functions, and the dynamical equations for the fluid simply become the equations for the trajectories of these vortices. The discrete-vortex model is essentially identical to the guiding-centre model for charged rods.

We can compute the electric field at the location of a particular rod ($\mathbf{E}_j$) due to the charge of all the others, and rewrite (4) as

$$\frac{d\mathbf{x}_i}{dt} = \sum_{j \neq i} \frac{\mathbf{K}_j}{2\pi} \times \frac{\mathbf{x}_{ij}}{x_{ij}^2}, \tag{5}$$

where $\mathbf{K}_j = -\lambda_j \mathbf{B}/\varepsilon_0 B^2$ and λ_j is the charge per unit length of the jth rod. It turns out that (5) is exactly the equation of motion for a line-vortex system (a system of delta functions in vorticity), with $\mathbf{K}_j$ representing the strength of the jth vortex (Onsager 1949). Henceforth, we can use the language of guiding-centre plasmas and vortex dynamics interchangeably. Indeed, practitioners of pure electron guiding-centre plasmas often refer to a column of electrons as a lump of vorticity.

The unusual properties of Navier–Stokes flow constrained to two dimensions were first noticed by Onsager (1949) and Fjortoft (1953). Onsager reduced the problem to one of an interaction of discrete line vortices very similar to the two-state spin problem. It was Onsager who first suggested the existence of a negative-temperature state above some critical energy and posited that the negative temperature state admitted no uniform, quiescent thermodynamic equilibrium. Fjortoft noticed that since both the mean square velocity (the energy) and the mean square vorticity (the enstrophy) were conserved, a transfer of $\langle v^2 \rangle$ to small scales must be accompanied by a transfer of $\langle v^2 \rangle$ to large scales. There are a number of references on 2D Navier–Stokes flows that have a review character, including Montgomery (1975, 1977, 1991*b*), Kraichnan and Montgomery (1980) Hasagawa (1985) and Chorin (1994).

3.1. Theoretical constructs: selective decay and maximal entropy

The curl of the Navier–Stokes equation for a two dimensional fluid can be written as

$$\frac{\partial \boldsymbol{\omega}}{\partial t} + \mathbf{v} \cdot \boldsymbol{\nabla} \boldsymbol{\omega} = \nu \nabla^2 \boldsymbol{\omega}, \tag{6}$$

where $\boldsymbol{\omega} = \omega \hat{\mathbf{z}} = \boldsymbol{\nabla} \times \mathbf{v}$ is the vorticity. Since $\mathbf{v} = (v_x, v_y, 0)$ and is divergence-free, we can write $\mathbf{v} = \hat{\mathbf{z}} \times \boldsymbol{\nabla} \psi$, so that $\omega = \nabla^2 \psi$, where ψ is the stream function. The vorticity can be thought of a source for the velocity field (just as J is a source for B in electrodynamics). Notice that for the guiding-centre plasma $\mathbf{v} = \hat{\mathbf{z}} \times \boldsymbol{\nabla} \phi / B_z$ and $\nabla^2 \phi = qn/\varepsilon_0$, so that the electrostatic potential ϕ plays the role of the stream function ψ and the charge density n plays the role of the vorticity ω.

Two ideal invariants of interest are the mean square velocity (energy per unit mass) and mean square vorticity (called the enstrophy), defined in configuration space:

$$E = \frac{1}{2}\int v^2\, d^2x, \qquad \Omega = \frac{1}{2}\int \omega^2\, d^2x. \tag{7}$$

Notice that since $\boldsymbol{\omega} = \nabla \times \mathbf{v}, \Omega(k)$, has two extra factors of k in Fourier space.

A model that is a precursor of selective decay is the absolute equilibrium ensemble model of ideal flow (Kraichnan 1967). In this statistical mechanical model, the phase space consists of a large but finite number of discrete Fourier modes, and the energy and enstrophy are exactly conserved. The equilibrium spectral predictions are

$$E(k) = \frac{1}{\alpha + \beta k^2}, \qquad \Omega(k) = \frac{k^2}{\alpha + \beta k^2}, \tag{8}$$

where α and β are inverse temperatures associated with E and Ω. Because β is always negative for large systems, the energy tends to be concentrated at the longest allowed wavelength (lowest k). This suggests, for the non-equilibrium case, a tendency for the nonlinear interactions to 'back-transfer' energy in k-space. This must be accompanied by a 'forward transfer' of enstrophy to higher k. The absolute equilibrium ensemble introduces a model with a finite number of degrees of freedom and a discretization in k space, a procedure that is clearly complementary to the discretization in real space that is central to the maximal entropy methods. However, the k-space methods introduce no correlation between distinct k-modes, and therefore cannot produce coherent real-space structures except those implied by the finite size of the periodic box (or container).

Notice also that whatever the spectrum of $E(k)$ happens to be, the extra factor of k^2 forces the spectrum of $\Omega(k)$ to peak at higher k (smaller scales), so that the effect of dissipation on $\Omega(k)$ is greater than on $E(k)$. This is the motivation for selective decay of enstrophy with respect to energy in 2D Navier–Stokes flows. In addition, it can be shown that the ratio of enstrophy to energy monotonically decays in time under the influence of 2D Navier–Stokes dynamics (Ting *et al.* 1986)

Formally, we which to extremize Ω subject to the constraint that E is conserved:

$$\delta\Omega - \lambda\, \delta E = 0, \tag{9}$$

where λ is a Lagrange multiplier (the enstrophy-to-energy ratio). Using (7), (9) becomes

$$\delta \int (\nabla \times \mathbf{v})^2\, d^2x - \lambda\delta \int v^2\, d^2x = 0. \tag{10}$$

Integrating by parts, we find

$$\int \delta\mathbf{v} \cdot (\nabla \times \nabla \times \mathbf{v} - \lambda\mathbf{v})\, d^2x + \oint (\delta\mathbf{v} \times \boldsymbol{\omega}) \cdot dl = 0. \tag{11}$$

If the boundary is such that the vorticity vanishes (free-slip or viscous) then the boundary term vanishes and we have the Euler equation for selective decay of enstrophy to energy in 2D Navier–Stokes flow:

$$\nabla \times \nabla \times \mathbf{v} = \nabla \times \boldsymbol{\omega} = \lambda\mathbf{v}, \tag{12}$$

or, written in terms of the stream function ψ,

$$\nabla^2\psi + \lambda\psi = 0. \tag{13}$$

In a Cartesian geometry, the selective decay solution takes the form

$$\psi(x, y) = \psi_0 \cos(k_x x) \cos(k_y y) \tag{14}$$

for some fixed $\mathbf{k} = (k_x, k_y)$. This is known as a 'single-wavenumber' state. Clearly the state that minimizes $\mathbf{\Omega}/E$ is the single-wavenumber state with the minimum $k = (k_x^2 + k_y^2)^{1/2}$ allowed by the boundary conditions.

To determine the state consistent with maximal entropy, we take our cue from the two-state spin system discussed in Sec. 2 and Boltzmann statistics. A statistical mechanical description of a continuum system requires that some kind of quantization be made. We consider the 2D fluid modelled by an array of N line vortices with n_+ clockwise and n_- counterclockwise (Onsager 1949; Joyce and Montgomery 1973). The entropy of such an array can be written (in analogy to (2)) as

$$S \equiv -\int n_+ \ln n_+ \, d^2x - \int n_- \ln n_- \, d^2x, \tag{15}$$

where now n_+ and n_- refer to the continuous two-dimensional number densities of clockwise and counterclockwise vortex distributions. We now want to maximize S subject to the constraints that the total energy and total number of entities are conserved. Note that the energy is purely potential energy due to the interaction of the vortices of fluid or rods of charge; there is no kinetic energy in the problem. As in the two-state spin system, the critical energy above which temperatures are negative is $E = 0$ (once the self-energy of the vortices or line charges has been subtracted). Maximizing (15) subject to the constraints that the total potential energy and the total vorticities of either sign ($\int n_+ \, d^2x$ and $\int n_- \, d^2x$) are conserved yields

$$N_\pm(x) = \exp[-\alpha_\pm \mp \beta\psi(x)], \tag{16}$$

where

$$\psi(x) = K \int \hat{\psi}(x, x')[n_+(x') - n_-(x')] \, d^2x, \tag{17}$$

with $\hat{\psi}(x, x')$ defined by $\nabla^2\hat{\psi} = -\delta(x - x')$ and $\alpha^\pm$ and β the Lagrange multipliers in the problem. By adding and subtracting the two equations in (16), combining $\alpha_\pm$ and K into a single constant λ and invoking the equations of constraint, we find the Montgomery–Joyce (or sinh–Poisson) equation:

$$\nabla^2\psi + \lambda^2 \sinh \mid \beta \mid \psi = 0. \tag{18}$$

It is useful to note here that $\sinh \psi \approx \psi$ to leading order, so that the result of the maximal-entropy principle can be viewed as a correction to the result of selective decay, (13), though the results come from very different physical viewpoints.

Detailed comparisons of the results of relaxation in 2D NS turbulence to the predictions of selective decay, (13), and of maximal entropy, (18), have been performed computationally (Matthaeus *et al.* 1991*a*, *b*; Montgomery *et al.* 1992, 1993). The 2D Navier–Stokes equation (6) was solved numerically in the Fourier representation with high resolution, and the dynamics was followed for nearly 400 characteristic times (eddy turnover time) (see Fig. 2). By the end of the simulation, only 1% of the initial enstrophy remained, while over 80% of the initial energy remained, clearly demonstrating the principle of selective decay. However, when we compare the correlations between the Navier–Stokes solution and the prediction of selective decay, $C(\omega, \psi)$, with that of the Navier–Stokes solution and the prediction of maximal

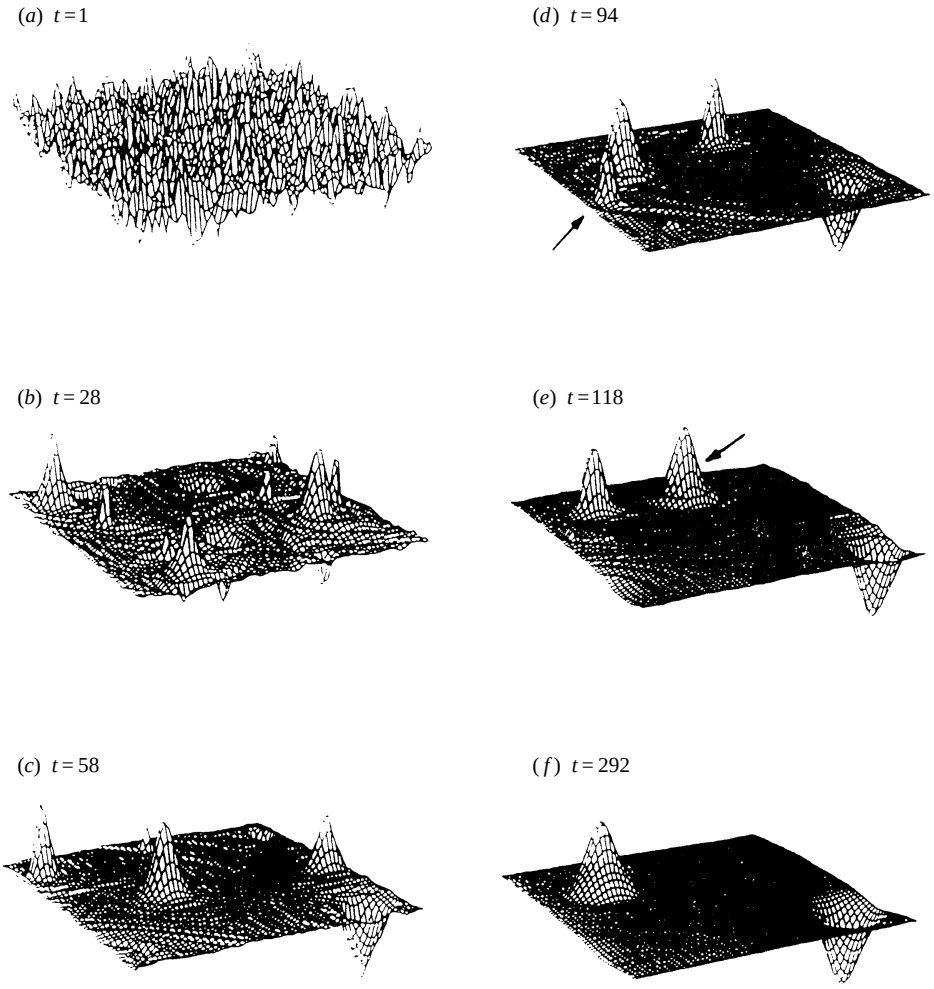

Figure 2. 3D perspective plots of the vorticity versus x and y for six successive times from a 2D Navier–Stokes simulation. (From Matthaeus *et al.* (1991).)

entropy, $C(\omega, \sinh \beta\psi)$, we find that maximal entropy is a much better predictor of the relaxed state (see Fig. 3). The astonishing point here is that a zero-dissipation, discrete model (maximal entropy) is a better predictor of relaxed states in viscous 2D NS turbulence than is a finite-dissipation, continuum model (selective decay).

3.2. Experimental evidence of relaxation in 2D fluid systems

Because of the direct correspondence between the 2D Navier–Stokes equation and the equation of motion for a guiding-centre plasma, some of the best experimental evidence of relaxation to large-scale structures comes from the UCSD pure-electron plasma group (Driscoll and Fine 1990; Mitchell *et al.* 1993; Huang and Driscoll 1994; Huang *et al.* 1995; Fine *et al.* 1995). The pure-electron plasmas are generated by hot filaments and trapped in a grounded cylinder. A strong, uniform axial magnetic field provides radial confinement, and negative voltages applied to cylindrical end electrodes provide the axial confinement. A typical experiment consists of injecting

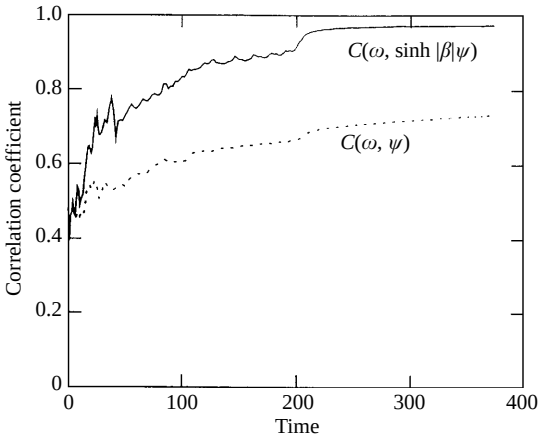

Figure 3. Evolving spatially averaged correlations between the relaxed state and the maximal-entropy prediction (——) and the selective-decay prediction (· · · · · ·) for the run depicted in Fig. 2. It is clear that the maximal-entropy hypothesis is a better fit. (From Matthaeus *et al.* (1991).)

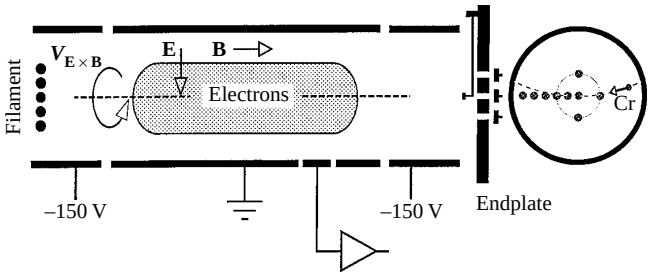

Figure 4. Schematic of the pure-electron guiding-centre plasma device. (From Huang and Driscoll (1994).)

a column (or several columns) of electrons into the cylindrical trap, allowing the system to evolve or relax, and then dumping the electrons out one end to be detected with electrostatic analysers or imaged on a phosphor screen (see Fig. 4).

The pure-electron plasmas typically have density $n_e \leqslant 10^7$ cm^{-3} and are confined in an axial field of a few hundred gauss and an axial potential well of a few hundred volts. The electron columns are about 1 cm in diameter and up to 40 cm long. The characteristic drift time of a column is about 10 μs while the viscous dissipation time is 10 s indicating that the effective Reynolds number is large (perhaps 10^6 or more). The electron cyclotron time is about 1 ns, so that the guiding-centre approximation is justified.

In a particularly interesting experiment, Driscoll and Fine (1990) and Fine *et al.* (1991) trapped two electron columns (vortices), and observed their merging in less than one rotation period (about 50 μs) (see Fig. 5). They noticed that the merging time is a strong function of the vortex separation. If the separation was increased from 1.8 to 2.0 diameters, the merging time increased from 10 μs to 1 s. The final single-vortex state has also been studied in detail with an array of electrostatic analysers (Huang and Driscoll 1994). In addition to these vortex-dynamics exper-

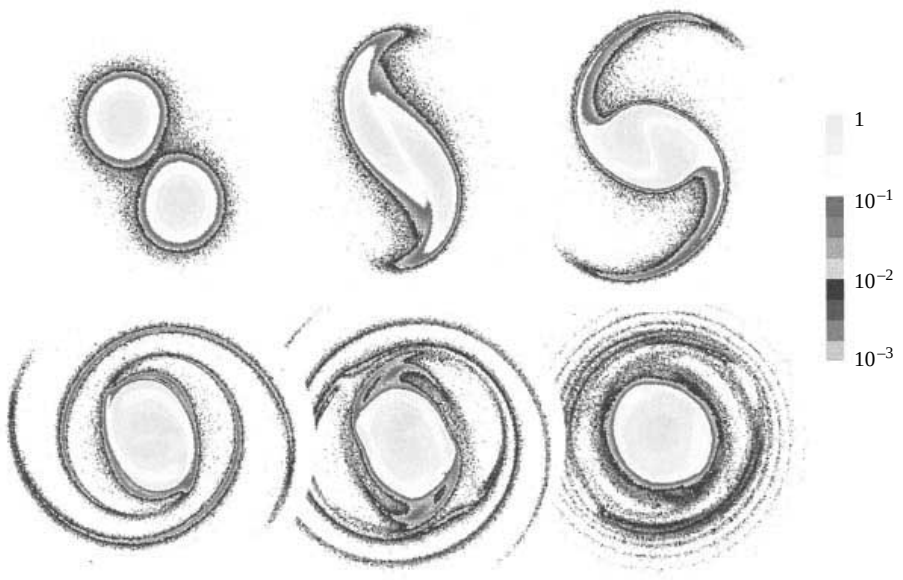

Figure 5. Merger of two pure-electron columns (vortices). Time intervals are 10 μs.(From Driscoll and Fine (1990).)

iments, the free relaxation of turbulent flows has been studied with a variety of initial conditions and detection techniques. Huang and Driscoll (1994) observed relaxation of an initially hollow vorticity profile, which is unstable to low-order azimuthal asymmetries. The profile of the relaxed state $n(r)$ is compared with the predictions of selective decay and maximal entropy, and a better fit is claimed with the selective decay state (see Fig. 6). Note that if $n_+ = N$ and $n_- = 0$ then fits should be to solutions of $\nabla^2\psi + \lambda^2 \exp(-\beta\psi) = 0$. However, fits of data to predictions of selective decay and maximal entropy and comparison of the results are subtle.

Experiments have also been performed on the free decay of turbulence characterized by 50–100 initial vorticies (Fine *et al.* 1995). The columns are formed by the rapid breakup of a helical sheet of charge due to the Kelvin–Helmholtz instability. Depending on subtleties of the initial conditions (not fully understood), the random-looking distribution of vorticity will either collapse to a single vortex or to a long-lived array of 'vortex crystals' (see Fig. 7). Given the foregoing discussion, the final single-vortex state is understandable in terms of either selective decay or maximal entropy; the vortex-crystal state is more difficult to understand. It is interesting to speculate whether conventional 2D fluids could exhibit vortex-crystal behaviour either experimentally or computationally.

Self-organization has been observed in the dynamics of quantized vortices in liquid ^{4}He. Yarmchuk *et al.* (1979) and Yarmchuk and Packard (1982) employed photographic techniques to image the vortex dynamics. Ions injected into the flow are attracted to vortex cores and accumulate there for several seconds. An applied electric field accelerates charge out of the vortices, where it is imaged on a phosphor screen. Single-vortex states have been observed, as well as arrays of 'vortex crystals' similar to those observed in pure-electron plasmas. A typical vortex has a diameter of 100 μm, and up to 11 have been observed in a single array. The diameter of the

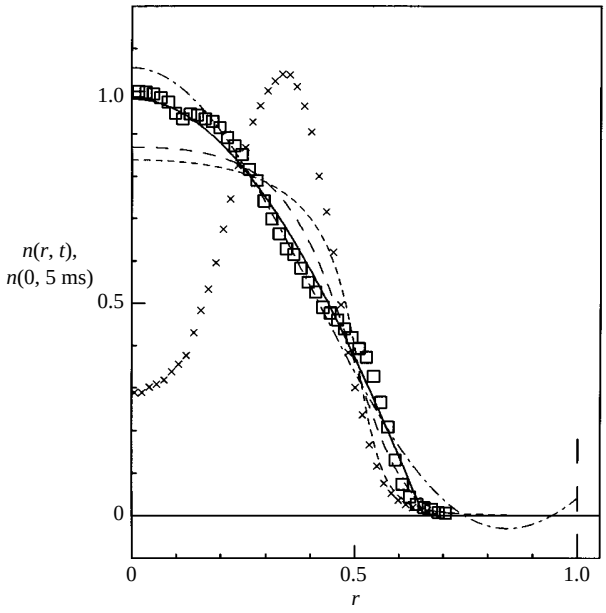

Figure 6. Measured radial density profiles of the initial (t = 0, ×) and metaequilibrium (t = 5 ms, □) states, and theoretical predictions from four models: ——, restricted minimal-entrophy; — - —, global minimum-entrophy; — —, plasma vortex maximal entropy; - - - -, fluid maximal-entropy. (From Huang and Driscoll (1994).)

tank was 2 mm. Note that the flow in this case is essentially dissipationless, so that we might expect the principle of maximal entropy to apply.

Griffiths and Hopfinger (1987) observed the merging of two vortices in rotating cylinders. Experiments were carried out in a 1 m diameter tank 0.2 m deep. Figure 8 depicts the merger of two vortices of differing strength. Note the qualitative similarity of merging of vortices in water to the merging of guiding-centre pure-electron plasmas in Fig. 5. It is also interesting to compare Figs 5 and 8 with a simulation of a vortex merger (McWilliams 1984) (see Fig. 9).

Gharib and Derango (1989) used a novel high-speed soap-film device to observe the dynamics of two-dimensional Navier-Stokes flow. A 4 in wide sheet of soap is pulled along parallel rods at velocities up to 2.5 m s^{-1} by the contact action of a two-dimensional water jet. The ratio of a typical transverse dimension to the thickness of the layer is about 10^4, ensuring a high degree of two-dimensionality. The Reynolds number can be varied up to about 10^4. Figure 10 depicts freely decaying 2D turbulence behind a grid placed in the flow. Notice that the average size of vortices increases downstream of the grid.

Tabeling *et al.* (1991) and Cardoso *et al.* (1994) observed relaxation in freely decaying two-dimensional turbulence using a thin layer of electrolyte. An array of counter-rotating vortices is established by driving a current across the layer with an array of permanent magnets below. $\mathbf{J} \times \mathbf{B}$ forces in the fluid establish a steady state of 100 vortices. When the current is turned off, the vortices begin to merge as the 2D fluid relaxes (Fig. 11). Tabeling *et al.* find that after a short time (0.7 s), the number of vortices is reduced by half, but the energy of the flow is approximately conserved ($E_{\text{fin}}/E_{\text{initial}} = 0.8$) (Fig. 12). The ratio of a typical transverse dimension to the thickness of the layer is about 10. The Reynolds number is between 600

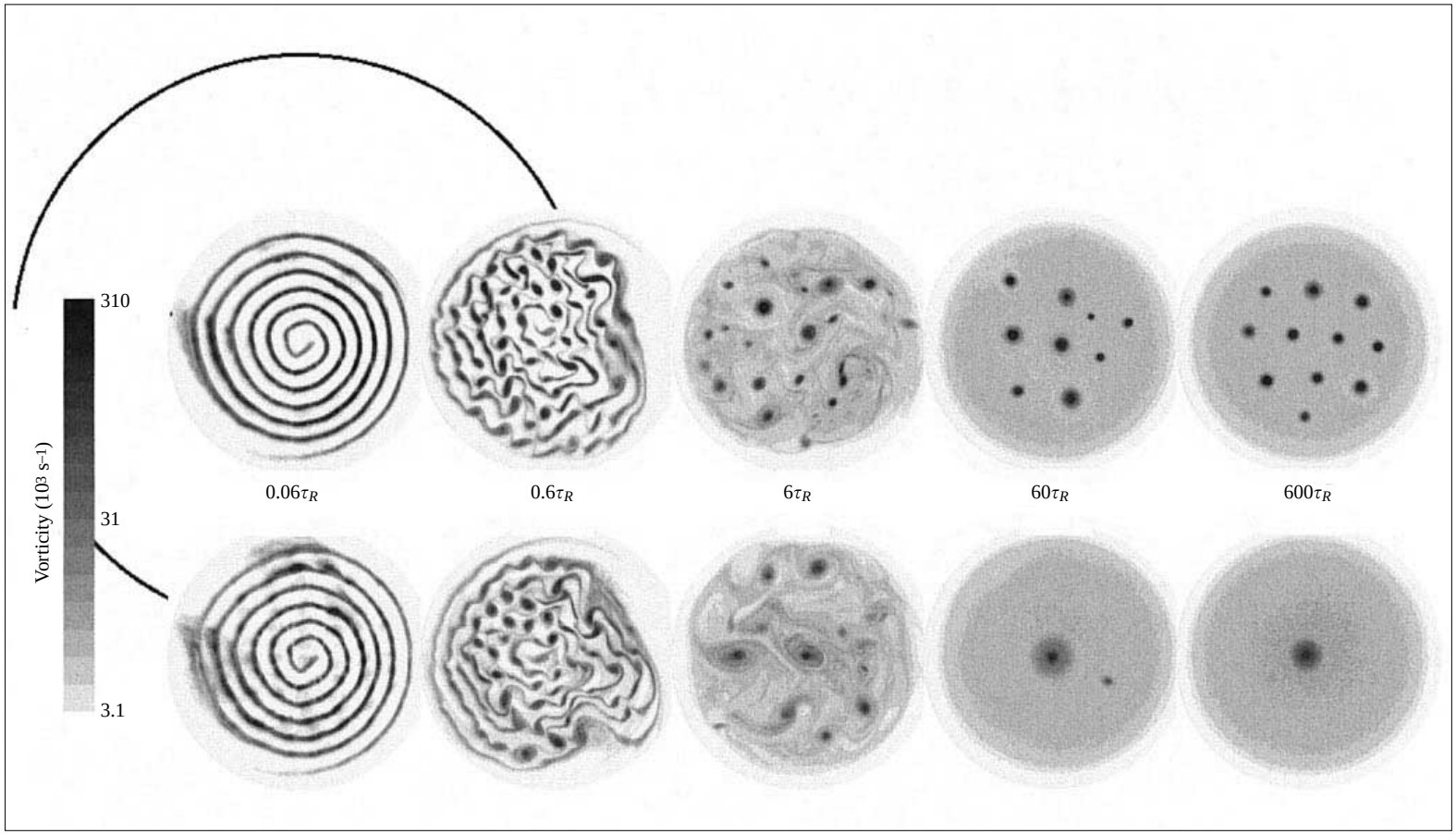

Figure 7. Images of vorticity at five times for two sequences from similar initial conditions. The black arcs indicate the wall radius. (From Fine *et al.* (1995).)

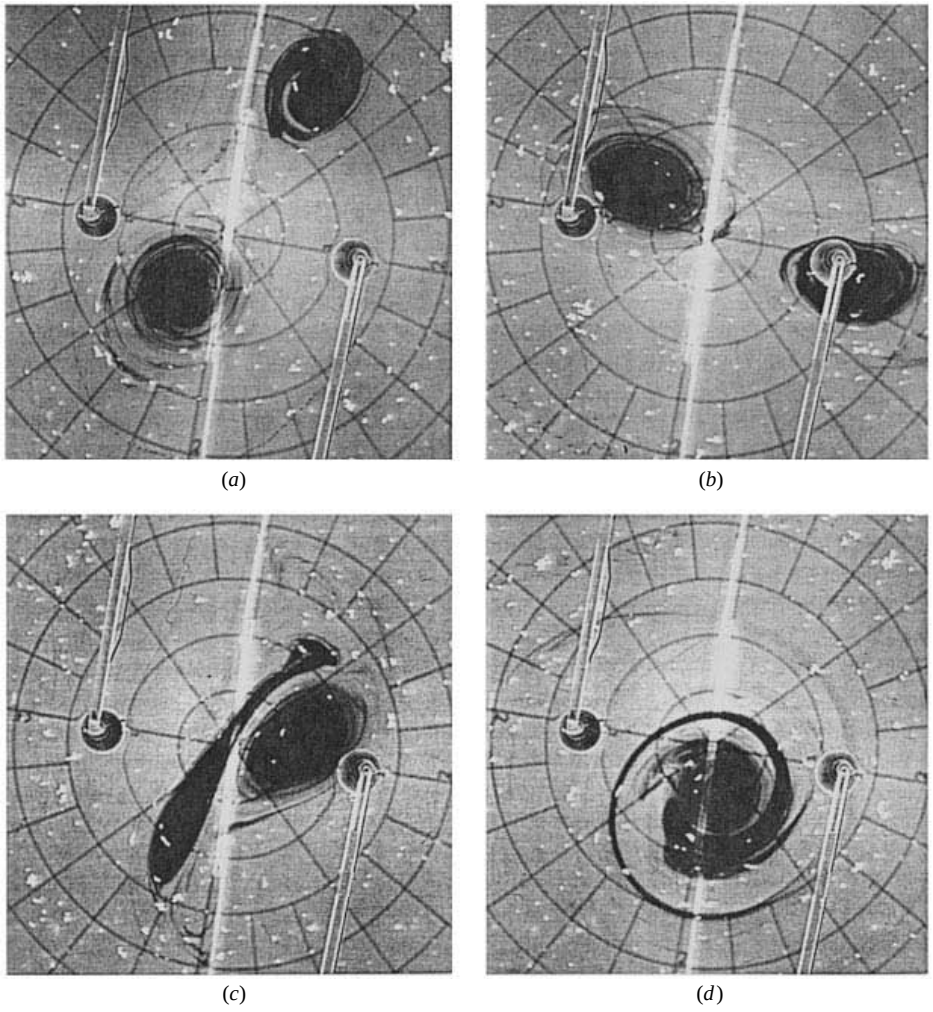

Figure 8. Merger of two vortices of differing strengths in a rotating water cylinder. Time intervals are 10 rotation periods; one period is about 6 s. (From Griffiths and Hopfinger (1987).)

and 2400. Notice the similarity among the images of freely decaying 2D turbulence depicted in Figs 7, 10 and 11.

4. Magnetohydrodynamics

A magnetofluid is an electrically conducting fluid obeying the laws of magnetohydrodynamics (MHD):

$$\rho\left(\frac{\partial \mathbf{v}}{\partial t} + \mathbf{v}\cdot\nabla\mathbf{v}\right) = -\nabla p + \mathbf{J}\times\mathbf{B} + \rho\nu\nabla^2\mathbf{v}, \tag{19}$$

$$\mathbf{E} + \mathbf{v}\times\mathbf{B} = \eta\mathbf{J}, \tag{20}$$

$$\frac{\partial \mathbf{B}}{\partial t} = \nabla\times(\mathbf{v}\times\mathbf{B}) + \frac{\eta}{\mu_0}\nabla^2\mathbf{B}, \tag{21}$$

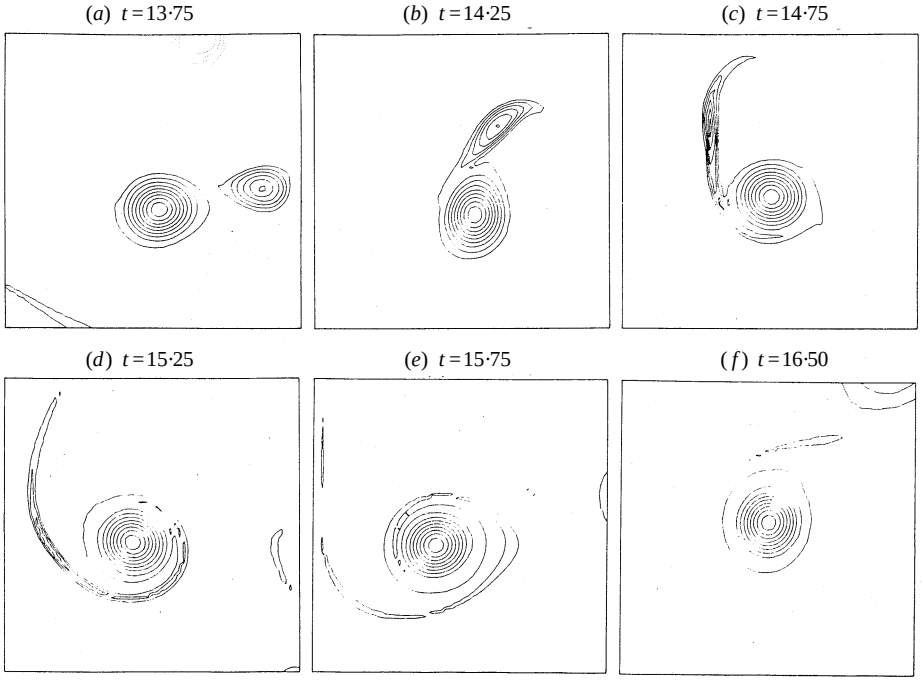

Figure 9. Merger of two vortices of differing strengths from a 2D Navier–Stokes simulation. (From McWilliams (1984).)

Figure 10. Two dimensional grid turbulence on a moving soap film. Notice the evidence of vortex merger downstream. (From Gharib and Derango (1989).)

where (19) is the equation of motion, (20) is Ohm's law and (21) is the curl of (20). Two ideal invariants of interest in the case of 3D MHD are the energy and magnetic helicity:

$$E_B = \int \frac{B^2}{2\mu_0}\, d^3x, \qquad K = \int \mathbf{A}\cdot\mathbf{B}\, d^3x, \tag{22}$$

where $\mathbf{B} = \nabla \times \mathbf{A}$. A third invariant, the cross-helicity $H_c = \int \mathbf{v}\cdot\mathbf{B}\, d^3x$, will not be discussed here. The helicity is related to the product of linked fluxes (Moffatt 1978),

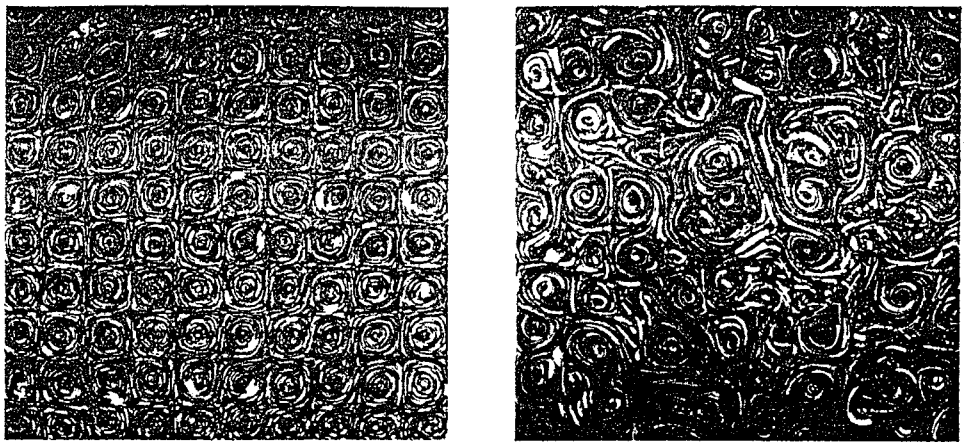

Figure 11. Freely decaying 2D turbulence from an initially ordered square lattice of 100 vortices in an electrolyte solution. The size of the system is 8 cm × 8 cm. (*a*) initial state at $t = 0$; (*b*) $t = 0.5$ s. (From Tabeling *et al.* (1991).)

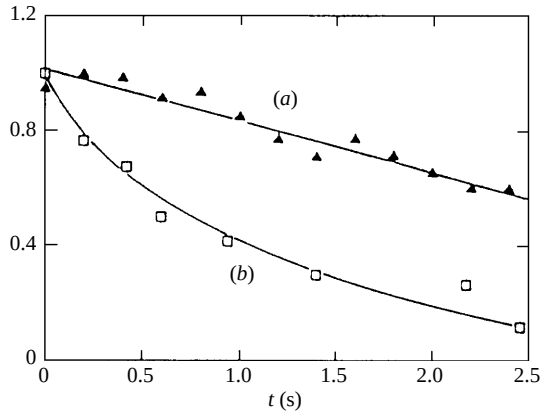

Figure 12. Temporal evolution of the spatially averaged velocity (*a*) and the number of remaining vortices $N - N_f$. (*b*) Both plots are normalized. (From Tabeling *et al.* (1991).)

and acts as a topological invariant. If the helicity is fixed then the magnetic energy cannot drop below a certain value without unlinking flux tubes. By the Schwartz triangle inequality, we can write (Frisch *et al.* 1975)

$$K^2 = \left(\int \mathbf{A} \cdot \mathbf{B} \, d^3x \right) \leqslant \left(\int A^2 \, d^3x \right) \left(\int B^2 \, d^3x \right), \tag{23}$$

and by the Poincaré inequality,

$$\int B^2 \, d^3x \geqslant \lambda^2 \int A^2 \, d^3x, \tag{24}$$

where λ is an inverse scale length in the system. Equations (23) and (24) together yield

$$E_B \geqslant \lambda \mid K \mid . \tag{25}$$

In other words, the magnetic energy is bounded from below owing to the magnetic helicity being conserved; E_B cannot decrease below some minimum value as long as K is finite. As we have seen in earlier sections, a bound on the available phase space is a necessary criterion for the formation of large-scale structures. The statistical properties of ideal 3D MHD are discussed in detail by Stribling and Matthaeus (1990) and Frisch *et al.* (1975).

An additional point supporting the likelihood of the formation of large-scale structures in 3D MHD has been provided by Frisch *et al.* (1975). In an argument similar to that of Fjortoft (1953) for 2D NS flows, they note that simultaneous transfer of E_B and K to small scales is impossible. Consider a magnetofluid in an initial state characterized by two wavenumbers $\mathbf{p}$ and $\mathbf{q}$ ($p < q$), and suppose that the state is 'maximally helical' (i.e. equality holds in (25), so that $\lambda = k_{\min}$ in the Fourier representation). Now let this excitation be transferred entirely to a new wavenumber $\mathbf{k}$. Because of conservation of magnetic energy and magnetic helicity, we have

$$E_B(p) + E_B(q) = E_B(k), \tag{26}$$

$$K(p) + K(q) = K(k) = \frac{E_B(p)}{p} + \frac{E_B(q)}{q} = \frac{E_B(k)}{k}. \tag{27}$$

We see that k must be less than q and the transfer must be to larger scales or else the condition (25) is violated.

4.1. Two-dimensional MHD

If the flow is limited to two dimensions, the full MHD equations reduce to (Fyfe and Montgomery 1976, 1978; Fyfe *et al.* 1977*a*, *b*; Hossain *et al.* 1983, 1985; Hossain 1994)

$$\frac{\partial \boldsymbol{\omega}}{\partial t} + \mathbf{v} \cdot \boldsymbol{\nabla} \boldsymbol{\omega} = \mathbf{B} \cdot \boldsymbol{\nabla} \mathbf{j} + \nu \nabla^2 \boldsymbol{\omega}, \tag{28}$$

$$\frac{\partial \mathbf{a}}{\partial t} + \mathbf{v} \cdot \boldsymbol{\nabla} \mathbf{a} = \eta \nabla^2 \mathbf{a}, \tag{29}$$

where $\boldsymbol{\omega}$ (the vorticity as in the 2D NS case), $\mathbf{j}$ (the current density) and $\mathbf{a}$ (the vector potential) are vectors with only a z component. The ideal invariants of interest are the mean square vector potential ($\int a^2 \, d^2x$) and the energy per unit mass. 2D MHD serves as a useful bridge between 2D NS and 3D MHD. There aren't many experiments for which 2D MHD applies (see, however, Sommeria 1986). It turns out that the role of ideal invariants in 2D MHD is similar to 3D MHD (with the mean square vector potential playing the role of magnetic helicity), while the geometry and velocity field are similar to those in 2D NS. Large-scale structures have been observed in 2D MHD simulations (Hossain 1994). There is recent computational evidence that suggests that at early times, maximal entropy is a better predictor of relaxed states in 2D MHD than is selective decay (M. Hossain, private communication).

4.2. Three-dimensional MHD: selective decay and maximal entropy

We use the same kind of justification for applying selective decay to 3D MHD as we did for 2D Navier–Stokes flows. Again, the two ideal invariants of interest in

the case of 3D MHD are the energy and magnetic helicity:

$$E_B = \int \frac{B^2}{2\mu_0}\, d^3x, \qquad K = \int \mathbf{A}\cdot\mathbf{B}\, d^3x, \tag{30}$$

where $\mathbf{B} = \nabla \times \mathbf{A}$. The justification for ignoring the kinetic energy of the magnetofluid E_K is primarily to simplify the calculation. The ratio of kinetic to magnetic energy $\beta = E_K/E_B$ is usually small in laboratory magnetofluids, but there are relatively few direct measurements of the velocity field (however, see Tynan *et al.* 1992). There are recent calculations using models more general than MHD that minimize the total magnetofluid energy $E_K + E_B$ subject to the constraint that the generalized helicity is conserved (where A is replaced by $A + mv/q$) (Steinhauer and Ishida 1996). It will be important in the future to resist the temptation to ignore the velocity field and put it on the same footing as the magnetic field where it belongs.

Notice that in the Fourier representation $E_B(k)$ has one more factor of k than does $K(k)$. Whatever the spectrum of $K(k)$ happens to be, the extra factor of k forces the spectrum of $E(k)$ to peak at higher k (smaller scales) so that the effect of dissipation on $E(k)$ is greater than on $K(k)$. This is the motivation for selective decay of energy with respect to helicity in 3D MHD. Formally, we wish to extremize E subject to the constraint that K is conserved:

$$\delta E_B + \lambda\, \delta K = 0, \tag{31}$$

where λ is a Lagrange multiplier with the units of inverse length (the energy-to-helicity ratio). After substitutions and an integration by parts, the minimization condition can be written as

$$\int \delta\mathbf{A}\cdot(\nabla\times\mathbf{B} - \lambda\mathbf{B})\, d^3x + \oint (\delta\mathbf{A}\times\mathbf{B} - \tfrac{1}{2}\delta\mathbf{A}\times\mathbf{A})\cdot d^2\mathbf{x} = 0. \tag{32}$$

If the magnetofluid is in a perfectly conducting container then $\mathbf{B}\cdot\hat{\mathbf{n}} = 0$, and the surface integral in (32) vanishes. We are left with the Euler equation for selective decay of energy to helicity in 3D MHD:

$$\nabla\times\mathbf{B} = \lambda\mathbf{B}. \tag{33}$$

This is often referred to as the force-free state (since if $\mathbf{J}$ is proportional to $\mathbf{B}$ then $\mathbf{J}\times\mathbf{B} = 0$) or the Taylor (1974, 1986) state. If the magnetofluid is in a perfectly conducting cylindrical vessel, the lowest-order solutions are proportional to Bessel functions:

$$\mathbf{B}_z = \mathbf{B}_0\, J_0(\lambda r), \qquad \mathbf{B}_\theta = \mathbf{B}_0\, J_1(\lambda r), \qquad \mathbf{B}_r = 0. \tag{34}$$

In order to compute the entropy of a continuum magnetofluid, some kind of quantization of the field variables needs to be made. In a seminal paper, Montgomery *et al.* (1979) suggested quantizing the axial current density J_z and the axial magnetic field B_z of a magnetofluid in a perfectly conducting cylinder into discrete filaments and discrete field lines respectively. We can then imagine dividing the cross-section of the cylinder into bins and counting the discrete entities in each one. The number of current filaments and field lines in the ith bin are n_i^J and n_i^B respectively. Note that there are six field variables that we could choose to quantize (J_z, B_z, A_z, J_θ, B_θ, A_θ) and that any two will determine the other four. For example, one could imagine an interacting flux tube model involving the vector potential A. We can write down the entropy of this system (in analogy with the

spin system of (2) and the vortex system of (15)):

$$S \approx -\sum_i n_i^j \ln n_i^j - \sum_i n_i^B \ln n_i^B, \tag{35}$$

where the sum is taken over all the bins in the cross-section. Note that the bins are fixed in space (just as the spins were in Sec. 2), but since the filaments and field lines can move, the occupation number of a particular bin can vary as long as the total number of filaments and field lines is fixed. We now want to maximize S subject to whatever constraints we wish to impose. The constraint that the total number of filaments and field lines are fixed is tantamount to holding constant the axial current and flux:

$$I_z \propto \sum_i n_i^J = \text{const}, \tag{36}$$

$$\Phi_z \propto \sum_i n_i^B = \text{const}. \tag{37}$$

Since there is magnetic energy stored in both the axial field and the field due to the axial current, conservation of magnetic energy involves the squares of the n_i (again, kinetic energy is ignored to simplify the problem). If we also wish to fix the magnetic helicity, there will be a fourth constraint involving sums of the cross-product $n_i^J n_j^B$. Maximizing (35) subject to these four constraints yields the following expressions for the most probable distribution of the field variables (Montgomery *et al.* 1979):

$$B_z = \exp(-\alpha_B - \beta B_z - \gamma A_z), \tag{38}$$

$$J_z = \exp(-\alpha_J - \beta A_z - \gamma \pi), \tag{39}$$

where π is an auxiliary field related to B_z,

$$\pi = \int A(x, x') B_z(x')\, d^2x', \tag{40}$$

and A_z and $A(x, x')$ solve the Poisson equations $\nabla^2 A_z = -J_z$ and $\nabla^2 A = -\delta(x - x')$. The Lagrange multipliers α_J, α_B, β and γ are associated with holding fixed I_z, Φ_z, E_B and K respectively, and can be viewed as inverse (possibly negative) temperatures. Since E_B is bounded from below by K, it is the associated inverse temperature β that can be negative. Note that (38) and (39) have the familiar form of the Boltzmann factor (which is derived in exactly the same way), and are highly nonlinear since B_z and A_z appear in the exponent. An analogue to the Montgomery–Joyce maximal-entropy equation for 2D vortices, (18), can be obtained by substituting (39) into the Poisson equation for J_z:

$$\nabla^2 A_z = \exp(-\alpha_J - \beta A_z - \gamma \pi). \tag{41}$$

This equation is similar in form to the maximal-entropy equation for a single component guiding-centre plasma, though more unwieldy because of the auxiliary function π.

Ambrosiano and Vahala (1981) used the maximal-entropy states (38) and (41) to determine the most probable distributions of current in a tokamak and a reversed-field pinch. In the absence of flow, the equation of motion (19) reduces to one of pressure balance (called the Grad–Shafranov equation): $\mathbf{J} \times \mathbf{B} = \nabla P$. Ambrosiano and Valhala used the maximal-entropy states as a mechanism to select among the infinitely many solutions to the Grad–Shafranov equation. Recently, other authors

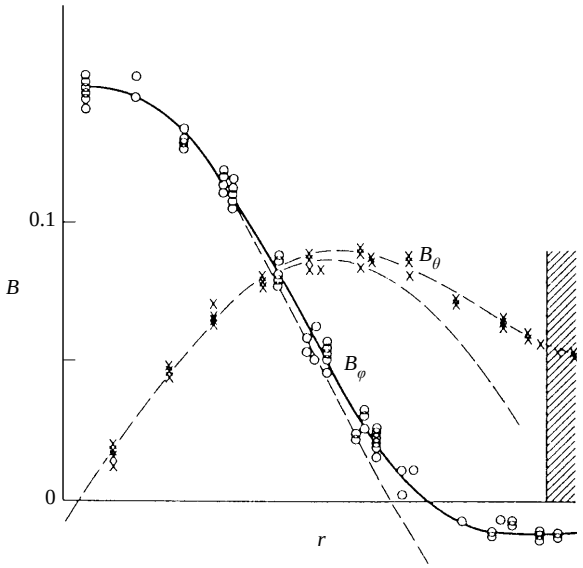

Figure 13. Experimental and theoretical (34) magnetic field profiles from the reversed-field pinch HBTX-1A. (From Bodin (1984).)

have adopted the notion of a magnetofluid composed of discrete filaments (Taylor 1993; Kinney *et al.* 1994).

4.3. Experimental evidence

There are relatively few direct measurements of magnetic fields and velocity fields in relaxed, un-driven 3D magnetofluids. To be of interest to the fusion program, tokamak magnetofluids require an externally applied electric field (for current drive), and generally have external sources of heat and particles. In addition, the tokamak is prevented from rapid relaxation by the application of a strong toroidal field. The major early success of the theory of selective decay of energy to helicity was applied by Taylor to relaxed reversed-field pinches and spheromaks (Taylor 1974, 1986). Figures 13 and 14 show the toroidal and poloidal field profiles from the reversed-field pinch HBTX-1A (Bodin 1984) and the spheromak Beta II (Turner *et al.* 1983) compared with the prediction of selective decay, i.e. the Bessel-function solution of the force-free state (33) and (34). The fit is clearly quite good, but departures from the Taylor force-free state have been noted in spheromaks (Knox *et al.* 1986).

The remarkable aspect of relaxation in 3D magnetofluids is the rapid time scale over which it occurs. Spheromak researchers have observed that spheromak relaxation to the selective decay Taylor state can occur within a few Alfvén transit times (Barnes *et al.* 1986; Jarboe 1994). Experiments have also been performed on the merging of separate spheromak and tokamak magnetofluids of the same sign of helicity (Brown and Bellan 1990*a*, *b*, 1992). Results show that the higher-helicity (higher-current) merged tokamak state is established in a few Alfvén times. If selective decay of energy to helicity was the only process at work in these experiments then we would expect that these large scale structures would evolve over the course of many Alfvén times rather than just one or two. It should be added here that rapid relaxation in decaying 3D magnetofluids has also been observed in simula-

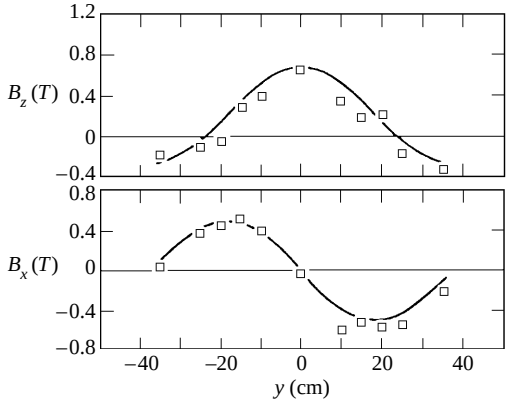

Figure 14. Experimental and theoretical (34) magnetic field profiles (poloidal component B_z and toroidal component B_x), from the spheromak Beta II. (From Turner *et al.* (1983).)

tions for some time (Riyopoulos *et al.* 1982; Dahlburg *et al.* 1986, 1987; Horiuchi and Sato 1985).

5. Discussion and conclusions

There is strong theoretical, computational and experimental evidence of rapid relaxation in continuous media and turbulent fluids. Experimental evidence from guiding-centre pure-electron plasmas and 3D magnetofluids is consistent with the selective-decay hypothesis. Theoretical and computational evidence from 2D Navier–Stokes turbulence and from 2D MHD suggest that the underlying principle driving the relaxation is maximal entropy as opposed to selective decay of one ideal invariant over another. The short time scale of the relaxation and the fit of the relaxed configuration to maximal entropy states provide the evidence.

The work of Montgomery and his collaborators indicates a different philosophical mind set from the historical trend of fusion research. Rather than focus attention on the fantastically complicated dynamics of turbulent fluids and magnetofluids, why not treat the 3D MHD system statistically and bring the enormous power of statistical mechanics and thermodynamics to the problem? It is conceivable that turbulent 3D MHD systems relax to a most probable (maximal-entropy) state subject to constraints on flux, current and ideal invariants in much the same way the air in a sealed room seeks the most probable state subject to constraints on particle number and energy.

In this light, there are several avenues for future work.

Maximal-entropy states for 3D MHD. It will be important to find maximal-entropy states for 3D MHD analogous to the Montgomery–Joyce sinh–Poisson maximal-entropy state demonstrated for 2D NS (perhaps using (41) as a start). The sinh-Poisson equation (from maximal entropy) proved to be an improvement to the Euler equation (from selective decay of enstrophy to energy) in 2D NS simulations. Might the force-free condition (the Euler equation from selective decay of energy-to-helicity) be improved upon by its discrete counterpart? It is well known, for example, that spheromaks only approximately relax to the Taylor or force-free

state. It is possible that spheromaks have instead relaxed to a maximal-entropy state.

The problem is complicated, since we are applying statistical mechanics to continuum systems. The magnetofluid will need to be quantized using discrete current filaments (Montgomery *et al.* 1979), quantized vector potential (Fyfe and Montgomery 1976, 1978; Fyfe *et al.* 1977*a*,*b*) or discrete flux bundles. Quantization by considering Fourier modes of the system is problematic, since a Fourier transform ignores phase relationships among the modes. Note that the Fourier transform of a coherent delta function and white noise are the same; organized, large-scale structures can have the same Fourier spectrum as fully developed turbulence.

Strictly speaking, maximal-entropy concepts only apply to isolated systems (e.g. freely decaying MHD systems). However, steady-state fusion devices will necessarily be attached to reservoirs of particles and energy. Perhaps it will be useful to focus on other thermodynamic potentials. For example, a system in contact with a heat reservoir at constant temperature will tend to minimize the Helmholtz free energy $F = E - TS$, and a system in contact with a reservoir at constant temperature and pressure will tend to minimize the Gibbs free energy $G = E - TS - PV$. In addition to seeking maximal-entropy states, it might be useful to consider minimal Helmholtz and Gibbs free-energy states.

The role of the velocity field in MHD. Experimentalists need to come to grips with the full implications of a 3D magnetofluid, including flow. As mentioned in Sec. 4.2, the justification for ignoring the kinetic energy and the velocity field in MHD calculations is weak. Grad–Shafranov equilibria in tokamaks and Taylor states in spheromaks ignore the velocity field. From a theoretical perspective, maximal-entropy states will likely include flow. From an experimental perspective, there is strong evidence that confined magnetofluids have large organized flows (for tokamaks, see Tynan *et al.* (1992), and for spheromaks, Peyser and Goldenbaum (1988) and Barrow and Goldenbaum (1990)). As pointed out by Frisch *et al.* (1975), if large-scale magnetic structures develop then large-scale velocity fields will necessarily be generated by the $\mathbf{J} \times \mathbf{B}$ term in the equation of motion (19). The inverse cascade then proceeds through the interaction of the velocity fields with the large-scale magnetic fields. To make matters worse, there is an inconsistency between the selective decay Taylor state and the stipulation of no flow (D. Montgomery, private communication). If there is no flow and if the magnetofluid is in steady state then Ohm's and Faraday's laws reduce to

$$\mathbf{E} = \eta \mathbf{J}, \qquad \nabla \times \mathbf{E} = 0. \tag{42}$$

The Euler equation for selective decay of energy to helicity (Taylor state) is

$$\nabla \times \mathbf{B} = \lambda \mathbf{B}, \qquad \text{or} \quad \mathbf{J} = \frac{\lambda}{\mu_0} \mathbf{B}. \tag{43}$$

Equations (42) and (43) are inconsistent, since

$$\nabla \times \mathbf{E} = \nabla \times (\eta \mathbf{J}) = \frac{\eta \lambda}{\mu_0} \nabla \times \mathbf{B} \neq 0, \tag{44}$$

unless η is identically zero.

Role of dissipation. Formation of large-scale structures often happens on time scales much shorter than dissipation time scales. Indeed, maximal-entropy theories have

no dissipation at all. It is clear that reconnection in 3D MHD and vortex merger in 2D NS require some dissipation. How is it that discrete, dissipationless models of relaxation are such good predictors of continuum, resistive reality?

Experimental tests. Wherever possible, experimental results should be compared with predictions of maximal entropy and selective decay. It has been demonstrated that 2D fluids relax to structures consistent with selective decay of enstrophy to energy (13) and that 3D magnetofluids relax to structures consistent with selective decay of energy to helicity, (33). However, these correspondences are far from exact. Computational evidence (at least for the case of 2D fluids) suggests that a better correspondence can be found with the Montgomery–Joyce equation of maximal-entropy states (18) (Matthaeus *et al.* 1991*a*)

Proof of H theorems. Finally, all arguments based on maximum entropy hinge on the assumption of an H theorem that says that the entropy (however we define it) tends to increase. H theorems exist for discrete systems, but no H theorem exists for continuous systems (see, however, Carnevale *et al.* 1981). It is important that H theorems be proved for 3D MHD as well as for 2D MHD and 2D NS.

Acknowledgements

The author gratefully acknowledges 10 years of guidance, discussions and apprenticeship with Professor David Montgomery, and wishes him all the best on the occasion of his 60th birthday. Discussions with Drs W. H. Matthaeus, M. Hossain, N. R. Corngold and P. J. Collings are also gratefully acknowledged. This work was supported by the DOE, the Research Corporation and the Petroleum Research Fund.

References†

Abragam, A. and Proctor, W. G. 1957 Experiments on spin temperature. *Phys. Rev.* **106**, 160.

Ambrosiano, J. and Vahala, G. 1981 Most probable magnetohydrodynamic tokamak and reversed field pinch equilibria. *Phys. Fluids* **24**, 2253.

Barnes, C. W., Fernandez, J. C., Henins, I., Hoida, H. W., Jarboe, T. R., Knox, S. O., Marklin, G. J. and McKenna. K. F. 1986 Experimental determination of the conservation of magnetic helicity from the balance between source and spheromak. *Phys. Fluids* **29**, 3415.

Barrow, B. and Goldenbaum, G. C. 1990 Mechanical injection of magnetic helicity during spheromak formation. *Phys. Rev. Lett.* **64**, 1369.

Bodin, H. A. B. 1984 *Proceedings of the International Conference on Plasma Physics, Lausanne*, (ed. M. Q. Tran and R. J. Verbeek), Vol. I, p. 417 EEC, Brussels.

Brown, M. R. and Bellan, P. M. 1990*a* Current drive by spheromak injection into a tokamak. *Phys. Rev. Lett.* **64**, 2144.

Brown. M. R. and Bellan, P. M. 1990*b* Spheromak injection into a tokamak. *Phys. Fluids* **B2**, 1306.

Brown, M. R. and Bellan, P. M. 1992 Efficiency and scaling of current drive and refueling by spheromak injection into a tokamak. *Nuc. Fusion* **32**, 1125.

† Campbell, L. J. and O'Neil, K. 1991 Statistics of two-dimensional point vortices and high energy vortex states. *J. Stat. Phys.* **65**, 495.

Cardoso, O., Marteau, D. and Tabeling, P. 1994 Quantitative experimental study of the free decay of quasi-two-dimensional turbulence. *Phys. Rev.* **E49**, 454.

† References relevant to the subject of this paper, but not directly cited in the text, are indicated with a dagger.

Carnevale, G. F., Frisch, U. and Salmon, R. 1981 H theorems in statistical fluid dynamics. *J. Phys. A: Math. Gen.* **14**, 1701.

Chorin, A. J. 1994 *Vorticity and Turbulence*. Springer-Verlag, New York.

Dahlburg, J. P., Montgomery, D., Doolen, G. D. and Turner, L. 1986 Turbulent relaxation to a force free field reversed state. *Phys. Rev. Lett.* **57**, 428.

Dahlburg, J. P., Montgomery, D., Doolen, G. D. and Turner, L. 1987 Turbulent relaxation of a confined magnetofluid to a force free state. *J. Plasma Phys.* **37**, 299.

Dahlburg, J. P., Montgomery, D., Doolen, G. D. and Turner, L. 1988 Driven, steady-state RFP computations. *J. Plasma Phys.* **40**, 39.

† Driscoll, C. F. 1990 Observation of an unstable $l = 1$ diocotron mode on a hollow electron column. *Phys. Rev. Lett.* **64**, 645.

Driscoll, C. F. and Fine, K. S. 1990 Experiments on vortex dynamics in pure electron plasmas. *Phys. Fluids* **B2**, 1359.

† Eyink, G. L. and Spohn, H. 1993 Negative temperature states and large scale, long lived vortices in two-dimensional turbulence. *J. Stat. Phys.* **70**, 833.

Fine, K. S., Driscoll, C. F. and Malmberg, J. H. 1991 Measurements of symmetric vortex merger. *Phys. Rev. Lett.* **67**, 588.

Fine, K. S., Cass, A. C., Flynn, W. G. and Driscoll, C. F. 1995 Relaxation of 2D turbulence to vortex crystals. *Phys. Rev. Lett.* **75**, 3277.

Fjortoft, R. 1953 On the changes in the spectral distribution of kinetic energy for two-dimensional non-divergent flow. *Tellus* **5**, 225.

Frisch, U., Pouquet, A., Leorat, J. and Mazure, A. 1975 Possibility of an inverse cascade of magnetic helicity in magnetohydrodynamic turbulence. *J. Fluid Mech.* **68**, 769.

Fyfe, D. and Montgomery, D. 1976 High beta turbulence in two-dimensional magnetohydrodynamics. *J. Plasma Phys.* **16**, 181.

Fyfe, D. and Montgomery, D. 1978 Statistical formulation of one-dimensional electron fluid turbulence. *Phys. Fluids* **21**, 316.

Fyfe, D., Joyce, G. and Montgomery, D. 1977*a* Magnetic dynamo action in two-dimensional turbulent magnetohydrodynamics. *J. Plasma Phys.* **17**, 317.

Fyfe, D., Montgomery, D. and Joyce, G. 1977*b* Dissipative, forced turbulence in two-dimensional magnetohydrodynamics. *J. Plasma Phys.* **17**, 369.

Gharib, M. and Derango, P. 1989 A liquid film soap film tunnel to study two-dimensional laminar and turbulent shear flows. *Physica* **D37**, 406.

Griffiths, R. W. and Hopfinger, E. J. 1987 Coalescing of geostrophic vortices. *J. Fluid Mech.* **178**, 73.

Hasagawa, A. 1985 Self-organization processes in continuous media. *Adv. Phys.* **34**, 1.

Horiuchi, R. and Sato, T. 1985 Three dimensional self organization of a magnetohydrodynamic plasma. *Phys. Rev. Lett.* **55**, 211.

† Hossain, M. 1991 Inverse energy cascades in three-dimensional turbulence. *Phys. Fluids* **B3**, 511.

Hossain, M. 1994 Anisotropy and inverse cascades in homogeneous turbulence. *Curr. Top. Phys. Fluids* **1**, 207.

Hossain, M., Matthaeus, W. H. and Montgomery, D. 1983 Long-time states of inverse cascades in the presence of a maximum length scale. *J. Plasma Phys.* **30**, 479.

Hossain, M., Vahala, G. and Montgomery, D. 1985 Forced magnetohydrodynamic turbulence in a uniform external magnetic field. *Phys. Fluids* **28**, 3074.

Huang, X. P. and Driscoll, C. F. 1994 Relaxation of 2D turbulence to a metaequilibrium near the minimum enstrophy state. *Phys. Rev. Lett.* **72**, 2187.

Huang, X. P., Fine, K. S. and Driscoll, C. F. 1995 Coherent vorticity holes from 2D turbulence decaying in a background shear flow. *Phys. Rev. Lett.* **74**, 4424.

Jarboe, T. R. 1994 Review of spheromak research. *Plasma Phys. Contr. Fusion* **36**, 945.

† Jarboe, T. R., Henins, I., Hoida, H. W., Linford, R. K., Marshall, J., Platts, D. A. and

† References relevant to the subject of this paper, but not directly cited in the text, are indicated with a dagger.

Sherwood, A. R. 1980 Motion of a compact toroid inside a cylindrical flux conserver. *Phys. Rev. Lett.* **45**, 1264.

† Jarboe, T. R., Henins, I., Sherwood, A. R., Barnes, C. W. and Hoida, H. W. 1983 Slow formation and sustainment of spheromaks by a coaxial magnetized plasma source. *Phys. Rev. Lett.* **51**, 39.

† Jarboe, T. R., Wysocki, F. J., Fernandez, J. C., Henins, I. and Marklin, G. J. 1990 Progress with energy confinement time in the CTX spheromak. *Phys. Fluids* **B2**, 1342.

† Joyce, G. and Montgomery, D. 1972 Simulation of the negative temperature instability for line vortices. *Physics Lett.* **39A**, 371.

Joyce, G. and Montgomery, D. 1973 Negative temperature states for the two-dimensional guiding-center plasma. *J. Plasma Phys.* **10**, 107.

Kinney, R., Tajima, T., McWilliams, J. C. and Petviashvili, N. 1994 Filamentary magneto-hydrodynamic plasmas. *Phys. Plasmas* **1**, 260.

Knox, S. O., Barnes, C. W., Marklin, G. J., Jarboe, T. R., Henins, I., Hoida, H. W. and Wright, B. L. 1986 Observations of spheromak equilibria which differ from the minimum-energy state and have internal kink distortions. *Phys. Rev. Lett.* **56**, 842.

Kraichnan, R. H. 1967 Inertial ranges in two-dimensional turbulence. *Phys. Fluids* **10**, 1417.

Kraichnan, R. H. and Montgomery, D. 1980 Two-dimensional turbulence. *Rep. Prog. Phys.* **43**, 547.

McWilliams, J. C. 1984 The emergence of isolated vortices in turbulent flow. *J. Fluid Mech.* **146**, 21.

† McWilliams, J. C. 1990*a* The vortices of two-dimensional turbulence. *J. Fluid Mech.* **219**, 361.

† McWilliams, J. C. 1990*b* A demonstration of the suppression of turbulent cascades by coherent vortices in two-dimensional turbulence. *Phys. Fluids* **A2**, 547.

Matthaeus, W. H. and Montgomery, D. 1980 Selective decay hypothesis at high mechanical and magnetic reynolds nembers. *Ann. NY Acad. Sci.* **357**, 203.

† Matthaeus, W. H. and Montgomery, D. 1981 Nonlinear evolution of the sheet pinch. *J. Plasma Phys.* **25**, 11.

Matthaeus, W. H. and Montgomery, D. 1984 Dynamic alignment and selective decay in MHD. *Statistical Physics and Chaos in Fusion Plasmas* (ed. W. H. Horton and L. E. Reichl), p. 285. Wiley, New York.

Matthaeus, W. H., Stribling, W. T., Martinez, D., Oughton, S. and Montgomery, D. 1991*a* Selective decay and coherent vortices in two dimensional incompressible turbulence. *Phys. Rev. Lett.* **66**, 2731.

Matthaeus, W. H., Stribling, W. T., Martinez, D., Oughton, S. and Montgomery, D. 1991*b* Decaying two-dimensional, Navier–Stokes turbulence at very long times. *Physica* **D51**, 531.

† Melander, M. V., Zabusky, N. J. and McWilliams, J. C. 1988 Symmetric vortex merger in two dimensions: causes and conditions. *J. Fluid Mech.* **195**, 303.

† Miller, J. 1990 Statistical mechanics of Euler equations in two dimensions. *Phys. Rev. Lett.* **65**, 2137.

† Miller, J., Weichman, P. B. and Cross, M. C. 1992 Statistical mechanics, Euler's equation and Jupiter's Great Red Spot. *Phys. Rev.* **A45**, 2328.

Mitchell, T. B., Driscoll, C. F. and Fine, K. S. 1993 Experiments on stability of equilibria of two vortices in a cylindrical trap. *Phys. Rev. Lett.* **71**, 1371.

Moffatt, H. K. 1978 *Magnetic Field Generation in Electrically Conducting Fluids*. Cambridge University Press.

† Montgomery, D. 1972 Two-dimensional vortex motion and negative temperatures. *Phys. Lett.* **39A**, 7.

Montgomery, D. 1975 Strongly magnetized classical plasma models. *Plasma Physics: Les Houches 1972* (ed. C. DeWitt and J. Peyraud). Gordon and Breach, New York.

Montgomery, D. 1977 Implications of Navier–Stokes turbulence theory for plasma turbulence. *Proc. Indian Acad. Sci.* **86A**, 87.

† References relevant to the subject of this paper, but not directly cited in the text, are indicated with a dagger.

Montgomery, D. 1989 Relaxed states in driven, dissipative magnetohydrodynamics: helical distortions and vortex pairs. Presented at the University of Minnesota Colloquium, 'Trends in Theoretical Physics'.

† Montgomery, D. 1991*a* Comment on 'Negative temperature of vortex motion'. *Phys. Rev.* **A44**, 8437.

Montgomery, D. 1991*b* Turbulent relaxation and its by-products. Prepared for Proceedings of the American Mathematical Society Special Session on 'Mathematical Aspects of Turbulence', 18–20 January, 1991, San Francisco, CA (ed. M. S. Berger).

Montgomery, D. and Joyce, G. 1974 Statistical mechanics of negative temperature states. *Phys. Fluids* **17**, 1139.

† Montgomery, D. and Lee, Y. C. 1990 Statistical mechanical selection of the shapes of disk galaxies. *Astrophys. J.* **368**, 380.

† Montgomery, D. and Shan, X. 1994 Determination of current profiles in confined magnetofluids. *Comments Plasma Phys. Contr. Fusion* **16**, 35.

Montgomery, D., Turner L. and Vahala, G. 1978 Three-dimensional MHD turbulence in cylindrical geometry. *Phys. Fluids* **21**, 757.

Montgomery, D., Turner, L. and Vahala, G. 1979 Most probable states in magnetohydrodynamics. *J. Plasma Phys.* **21**, 239.

Montgomery, D., Matthaeus, W. H., Stribling, W. T. Martinez, D. 1992 Relaxation in two dimensions and the sinh–Poisson equation. *Phys. Fluids* **A4**, 3.

Montgomery, D., Shan, X. and Matthaeus, W. H. 1993 Navier–Stokes relaxation to sinh–Poisson states at finite reynolds numbers. *Phys. Fluids* **A5**, 2207.

Onsager, L. 1949 Statistical hydrodynamics. *Suppl. Nuovo Cim.* **6**, 279.

† Peurrung, A. J. and Fajans, J. 1993*a* A limitation to the analogy between pure electron plasmas and two-dimensional inviscid fluids. *Phys. Fluids* **B5**, 4295.

† Peurrung, A. J. and Fajans, J. 1993*b* Experimental dynamics of an annulus of vorticity in a pure electron plasma. *Phys. Fluids* **A5**, 493.

† Peurrung, A. J., Notte, J. and Fajans, J. 1993 Collapse and winding of an asymmetric annulus of vorticity. *J. Fluid Mech.* **252**, 713.

Peyser, T. and Goldenbaum, G. C. 1988 Plasma rotation during spheromak formation. *Phys. Rev. Lett.* **61**, 955.

† Pointin, Y. B. and Lundgren, T. S. 1976 Statistical mechanics of two-dimensional vortices in a bounded container. *Phys. Fluids* **19**, 1459.

† Pouquet, A., Lesieur, M., André, J. C. and Basdevant, G. 1975 Evolution of high Reynolds number two-dimensional turbulence. *J. Fluid Mech.* **72**, 305.

† Pouquet, A., Frisch, U. and Léorat, J. 1976 Strong MHD turbulence and the nonlinear dynamo effect. *J. Fluid Mech.* **77**, 321.

Purcell, E. M. and Pound, R. V. 1951 A nuclear spin system at negative temperature. *Phys. Rev.* **81**, 279.

Ramsey, N. F. 1956 Thermodynamics and statistical mechanics at negative absolute temperatures. *Phys. Rev.* **103**, 20.

Riyopoulos, S., Bondeson, A. and Montgomery, D. 1982 Relaxation toward states of minimum energy in a compact torus. *Phys. Fluids* **25**, 107.

† Seyler, C. E. 1974 Partition function for a two-dimensional plasma in the random-phase approximation. *Phys. Rev. Lett.* **32**, 515.

† Seyler, C. E. 1976 Thermodynamics of two-dimensional plasmas or discrete line vortex fluids. *Phys. Fluids* **19**, 1336.

† Seyler, C. E., Salu, Y., Montgomery, D. and Knorr, G. 1975 Two-dimensional turbulence in inviscid fluids or guiding center plasmas. *Phys. Fluids* **18**, 803.

† Smith, R. A. 1989 Phase transition behavior in a negative temperature guiding center plasma. *Phys. Rev. Lett.* **63**, 1479.

† Smith, R. A. 1991 Maximization of vortex entropy as an organizing principle in intermittent, decaying, two-dimensional turbulence. *Phys. Rev.* **A43**, 1126.

† References relevant to the subject of this paper, but not directly cited in the text, are indicated with a dagger.

† Smith, R. A. and O'Neil, T. 1990 Nonaxisymmetric thermal equilibria of a cylindrically bounded guiding center plasma or discrete vortex system. *Phys. Fluids* **B2**, 2961.

Sommeria, J. 1986 Experimental study of the two-dimensional inverse energy cascade in a square box. *J. Fluid Mech.* **170**, 139.

Steinhauer, L. C. and Ishida, A. 1996 Finite minimum energy states of a two fluid flowing plasma. Submitted to *Phys. Plasmas*.

Stribling, T. and Matthaeus, W. H. 1990 Statistical properties of ideal three-dimensional magnetohydrodynamics. *Phys. Fluids* **B2**, 1979.

Tabeling, P., Burkhart, S., Cardoso, O. and Willaime, H. 1991 Experimental study of freely decaying two-dimensional turbulence. *Phys. Rev. Lett.* **67**, 3772.

† Taylor, J. B. 1972 Negative temperatures in two-dimensional vortex motion. *Phys. Lett.* **40A**, 1.

Taylor, J. B. 1974 Relaxation of toroidal plasma and generation of reverse magnetic fields. *Phys. Rev. Lett.* **33**, 1139.

Taylor, J. B. 1986 Relaxation and magnetic reconnection in plasmas. *Rev. Mod. Phys.* **58**, 741.

Taylor, J. B. 1993 Filamentation, current profiles and transport in a tokamak. *Phys. Fluids* **B5**, 4378.

Ting, A. C., Matthaeus, W. H. and Montgomery, D. 1986 Turbulent relaxation processes in magnetohydrodynamics. *Phys. Fluids* **29**, 3261.

† Ting, A. C., Chen, H and Lee, Y. C. 1987 Exact solutions of nonlinear boundary value problem: the vortices of the two-dimensional sinh–Poisson equation. *Physica* **D26**, 37.

Turner, W. C., Goldenbaum, G. C., Granneman, E. H. A., Hammer, J. H., Hartman, C. W., Prono, D. S. and Taska, J. 1983 Investigations of the magnetic structure and the decay of a plasma gun generated compact torus. *Phys. Fluids* **26**, 1965.

Tynan, G. R., Schmitz, L., Conn, R. W., Doerner, R. and Lehmer, R. 1992 Steady-state convection and fluctuation-driven particle transport in the H-mode transition. *Phys. Rev. Lett.* **68**, 3032.

† Williamson, J. H. 1977 Statistical mechanics of a guiding center plasma. *J. Plasma Phys.* **17**, 85.

† Wysocki, F. J., Fernandez, J. C., Henins, I., Jarboe, T. R. and Marklin, G. J. 1990 Improved energy confinement in spheromaks with reduced field errors. *Phys. Rev. Lett.* **65**, 40.

Yarmchuk, E. J. and Packard, R. E. 1982 Photographic studies of quantized vortex lines. *J. Low Temp. Phys.* **46**, 479.

Yarmchuk, E. J., Gordon, M. J. V. and Packard, R. E. 1979 Observation of stationary vortex arrays in rotating superfluid helium. *Phys. Rev. Lett.* **43**, 214.

† References relevant to the subject of this paper, but not directly cited in the text, are indicated with a dagger.